



# Experimental demonstration of 72% reach enhancement of 3.6Tbps optical transmission system using mid-link optical phase conjugation

MOHAMMAD A. Z. AL-KHATEEB,<sup>1,\*</sup> MINGMING TAN,<sup>1</sup> MD. ASIF IQBAL,<sup>1</sup> ABDALLAH ALI,<sup>1</sup> MARY E. MCCARTHY,<sup>1,2</sup> PAUL HARPER,<sup>1</sup> AND ANDREW D. ELLIS<sup>1</sup>

<sup>1</sup>Aston Institute of Photonic Technologies (AIPT), Aston University, Birmingham, B4 7ET, UK

<sup>2</sup>Oclaro Technologies, Long Road, Paignton TQ4 7AU, UK

\*alkhamaz@aston.ac.uk

**Abstract:** We experimentally demonstrate nonlinear noise compensation in an optical phase conjugation assisted 1<sup>st</sup> order Raman amplified 30x30Gbaud DP-QPSK transmission system with a spectral efficiency of 3.6b/s/Hz. We show that by optimizing the link symmetry, even with only 1<sup>st</sup> order Raman amplification a single, mid-link, optical phase conjugation compensates for 90% of the signal-signal nonlinear interference resulting in a 2.3dB performance enhancement. We show that increasing the number of optical phase conjugations in the presence of 10% residual nonlinearity results in a reduction in the performance enhancement owing to an enhancement in the nonlinear noise generation efficiency of the system. We achieve a record 72% optical phase conjugation enabled reach enhancement of the 30x30Gbaud DP-QPSK signals.

© 2018 Optical Society of America under the terms of the [OSA Open Access Publishing Agreement](#)

**OCIS codes:** (060.4510) Optical communications; (070.5040) Phase conjugation; (190.4370) Nonlinear optics, fibers; (190.5650) Raman effect.

## References and links

1. K. Roberts, L. Strawczynski, M. O'Sullivan, and I. Hardcastle, "Electronic precompensation of optical nonlinearity," *IEEE Photonics Technol. Lett.* **18**(2), 403–405 (2006).
2. A. Yariv, D. Fekete, and D. M. Pepper, "Compensation for channel dispersion by nonlinear optical phase conjugation," *Opt. Lett.* **4**(2), 52 (1979).
3. X. Li, X. Chen, G. Goldfarb, E. Mateo, I. Kim, F. Yaman, and G. Li, "Electronic post-compensation of WDM transmission impairments using coherent detection and digital signal processing," *Opt. Express* **16**(2), 880–888 (2008).
4. D. Lavery, D. Ives, G. Liga, A. Alvarado, S. J. Savory, and P. Bayvel, "The Benefit of Split Nonlinearity Compensation for Single-Channel Optical Fiber Communications," *IEEE Photonics Technol. Lett.* **28**(17), 1803–1806 (2016).
5. R. Dar and P. J. Winzer, "On the Limits of Digital Back-Propagation in Fully Loaded WDM Systems," *IEEE Photonics Technol. Lett.* **28**(11), 1253–1256 (2016).
6. E. Temprana, E. Myslivets, V. Ataie, B. P. P. Kuo, N. Alic, V. Vusirikala, V. Dangui, and S. Radic, "Demonstration of Coherent Transmission Reach Tripling by Frequency-Referenced Nonlinearity Pre-compensation in EDFA-only SMF Link," in *ECOC 2016; 42nd European Conference on Optical Communication*, 2016, pp. 1–3.
7. A. D. Ellis, M. E. McCarthy, M. A. Z. Al-Khateeb, and S. Sygletos, "Capacity limits of systems employing multiple optical phase conjugators," *Opt. Express* **23**(16), 20381–20393 (2015).
8. M. H. Shoreh, "Compensation of nonlinearity impairments in coherent optical OFDM systems using multiple optical phase conjugate modules," *J. Opt. Commun. Netw.* **6**(6), 549–558 (2014).
9. M. A. Z. Al-Khateeb, M. A. Iqbal, M. Tan, A. Ali, M. McCarthy, P. Harper, and A. D. Ellis, "Analysis of the nonlinear Kerr effects in optical transmission systems that deploy optical phase conjugation," *Opt. Express* **26**(3), 3145–3160 (2018).
10. M. A. Z. Al-Khateeb, M. E. McCarthy, and A. Ellis, "Performance Enhancement Prediction for Optical Phase Conjugation in Systems with 100km Amplifier Spacing," in *Proc. European Conference and Exhibition on Optical Communication (ECOC)* (2017), p. Th.1.F.4.

11. A. D. Ellis, M. Tan, M. A. Iqbal, A. Z. A.-K. Mohammad, V. Gordienko, G. S. Mondaca, S. Fabbri, M. F. C. Stephens, M. E. McCarthy, A. Perentos, I. D. Phillips, D. Lavery, G. Liga, R. Maher, P. Harper, N. Doran, S. K. Turitsyn, S. Sygletos, and P. Bayvel, "4 Tb/s Transmission Reach Enhancement Using  $10 \times 400$  Gb/s Super-Channels and Polarization Insensitive Dual Band Optical Phase Conjugation," *J. Lightwave Technol.* **34**(8), 1717–1723 (2016).
12. K. Solis-Trapala, T. Inoue, and S. Namiki, "Signal power asymmetry tolerance of an optical phase conjugation-based nonlinear compensation system," in *2014 The European Conference on Optical Communication (ECOC)* (2014), p. 1–3 (We.2.5.4).
13. H. Hu, R. M. Jopson, A. H. Gnauck, S. Randel, and S. Chandrasekhar, "Fiber nonlinearity mitigation of WDM-PDM QPSK/16-QAM signals using fiber-optic parametric amplifiers based multiple optical phase conjugations," *Opt. Express* **25**(3), 1618–1628 (2017).
14. T. Umeki, T. Kazama, A. Sano, K. Shibahara, K. Suzuki, M. Abe, H. Takenouchi, and Y. Miyamoto, "Simultaneous nonlinearity mitigation in  $92 \times 180$ -Gbit/s PDM-16QAM transmission over 3840 km using PPLN-based guard-band-less optical phase conjugation," *Opt. Express* **24**(15), 16945–16951 (2016).
15. K. Solis-Trapala, M. Pelusi, H. N. Tan, T. Inoue, and S. Namiki, "Optimized WDM Transmission Impairment Mitigation by Multiple Phase Conjugations," *J. Lightwave Technol.* **34**(2), 431–440 (2016).
16. S. L. Jansen, D. Van Den Borne, P. M. Krummrich, S. Spalter, G.-D. Khoe, and H. De Waardt, "Long-haul DWDM transmission systems employing optical phase conjugation," *IEEE J. Sel. Top. Quantum Electron.* **12**(4), 505–520 (2006).
17. I. Phillips, M. Tan, M. F. Stephens, M. McCarthy, E. Giacomidis, S. Sygletos, P. Rosa, S. Fabbri, S. T. Le, T. Kanesan, S. K. Turitsyn, N. J. Doran, P. Harper, and A. D. Ellis, "Exceeding the Nonlinear-Shannon Limit using Raman Laser Based Amplification and Optical Phase Conjugation," in *Optical Fiber Communication Conference* (2014), p. M3C.1.
18. S. Namiki, H. N. Tan, K. Solis-trapala, and T. Inoue, "Signal-transparent wavelength conversion and light-speed back propagation through fiber," in *Optical Fiber Communication Conference 2016* (2016), pp. 9–11.
19. G. Gao, X. Chen, and W. Shieh, "Influence of PMD on fiber nonlinearity compensation using digital back propagation," *Opt. Express* **20**(13), 14406–14418 (2012).
20. M. E. McCarthy, M. A. Z. Al Kahteb, F. M. Ferreira, and A. D. Ellis, "PMD tolerant nonlinear compensation using in-line phase conjugation," *Opt. Express* **24**(4), 3385–3392 (2016).
21. D. Rafique and A. D. Ellis, "Impact of signal-ASE four-wave mixing on the effectiveness of digital back-propagation in 112 Gb/s PM-QPSK systems," *Opt. Express* **19**(4), 3449–3454 (2011).
22. M. A. Z. Al-Khateeb, M. McCarthy, C. Sánchez, and A. Ellis, "Effect of second order signal-noise interactions in nonlinearity compensated optical transmission systems," *Opt. Lett.* **41**(8), 1849–1852 (2016).
23. A. D. Ellis, M. E. McCarthy, M. A. Z. Al Khateeb, M. Sorokina, and N. J. Doran, "Performance limits in optical communications due to fiber nonlinearity," *Adv. Opt. Photonics* **9**(3), 429–503 (2017).
24. ITU-T, *Forward Error Correction for High Bit-Rate DWDM Submarine Systems, Recommendation (G.975.1)*.

## 1. Introduction

Nonlinear Kerr effects of optical fibers are considered to be a major limiting factor to the performance of long-haul optical fiber transmission systems. Nonlinearity compensation techniques have been studied to expand the performance, reach, or capacity of optical fiber transmission systems. Those techniques can be implemented in the digital domain [1] or in the optical domain [2]. Digital nonlinearity compensation can be implemented in the transmitter [1], receiver [3], or both [4]. However, performing nonlinearity compensation in the digital domain is unlikely to fully compensate the nonlinear noise [5], since the nonlinear interference from neighboring WDM channels can dominate the total nonlinear noise. Indeed, full signal-signal nonlinearity compensation can only be realized in the digital domain with frequency locked transceivers, full knowledge of link properties, and sufficient (currently prohibitively complex) computational capabilities [6]. Optical phase conjugation (OPC) is an inline all-optical signal processing technique that provides transparent dispersion and nonlinearity compensation [2] when deployed symmetrically once (mid-link OPC [2]) or multiple times (multi-OPC [7,8]) along the transmission link. Only partial nonlinearity compensation can be achieved in discretely amplified or distributed Raman amplified transmission systems with large amplifier (or Raman pump) spacing [9], especially for large bandwidth systems [10]. Full compensation of deterministic (signal-signal) nonlinear effects can be achieved when an OPC is deployed in a quasi-lossless distributed Raman amplified system, either using Raman fiber laser based amplification [11] or very short span lengths [12]. A number of OPC demonstrations for Raman amplified links have been reported recently, which either offered only moderate (<2dB) performance improvement [13–17],

required short (12km) Raman pump spacing [12,18], or employed second order pumping [11].

With ideal OPC based nonlinearity compensation the system becomes limited by either polarization mode dispersion (PMD) induced reduction of compensation efficiency [19,20], or ultimately nonlinear signal-noise interactions [7,21,22]. In such systems, the deployment of multiple OPCs is expected to improve the performance, either by restricting the impact of PMD, or providing partial compensation of nonlinear signal-noise interactions [23] giving a significant performance advantage. On the other hand, if an OPC assisted system is limited by the nonlinear signal-signal interactions, the deployment of multiple OPCs may diminish the performance enhancement achieved by a single, mid-link, OPC due to enhanced phase matching attributable to the in-line dispersion compensation provided by the OPC [9]. Unfortunately, to date, no Raman amplified system has achieved compensation for more than 80% of the signal-signal nonlinearity with a total signal bandwidth above 250 GHz and an amplifier spacing above 20km, and clear benefits of multiple OPCs remain elusive.

In this paper, we report an experimental demonstration of 72% reach enhancement achieved by dual-band mid-link OPC using only 1st order Raman amplification with both broad bandwidth (30x30Gbaud WDM DP-QPSK at a spectral efficiency = 3.6b/s/Hz) and moderate (50km) amplifier spacing. This represents the highest reported long-haul reach enhancement for an OPC based system. The dual-band, polarization insensitive OPC enables spectrally efficient and concurrent phase conjugation of two optical bands. Nevertheless, whilst the results correspond to compensating ~89% of the signal-signal nonlinearity, this is insufficient to observe the benefits of signal-noise nonlinearity compensation by multiple OPCs. Indeed, we show that whilst a mid-link OPC assisted system achieves 2.2dB performance enhancement for all channels simultaneously, two and three OPCs generate reduced performance enhancements of 1.6dB and 1.4dB, respectively.

## 2. Transmitter

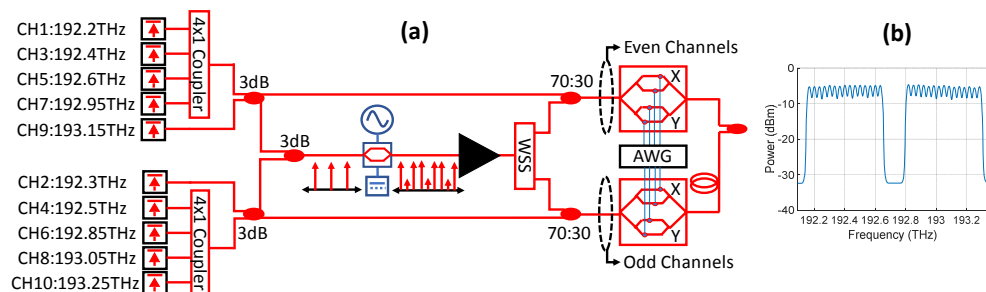


Fig. 1. (a) Experimental setup for spectrally efficient, comb-based transmitter system. (b) The optical spectrum of 30x30Gbaud DP-QPSK generated at the output of the transmitter. WSS: wavelength selective switch, AWG: arbitrary waveform generator.

In this experiment, we used 10 lasers (linewidth<100kHz), as shown in Fig. 1(a), where these lasers were spectrally divided between the two OPC bands (Band1:Ch1-5 and Band2:Ch6-10), and the spectral separation between neighboring lasers in each band was 100GHz. The even indexed lasers (Ch2, Ch4, Ch6, Ch8, Ch10) were combined using 4x1 and 2x2 couplers, as were the odd indexed lasers. The two sets of lasers were then further combined using a 3dB coupler to be modulated by an optical modulator fed by a 33GHz clock. The modulator suppresses the laser carrier and generated two optical tones (with 66GHz frequency separation) giving 20 optical lines at the output of the phase modulator. A 1x2 wavelength selective switch (WSS) was used to suppress the remaining unsuppressed carriers and segregate (to different output ports) the comb lines originated from even indexed lasers and the comb lines originated from odd indexed laser. Using a 70:30 optical coupler, the comb lines (at the output of the WSS) from even indexed lasers were combined with outputs of the

original odd indexed lasers, and vice versa. The resultant two sets of 15 optical spectral lines separated by 66GHz (in each band) were then separately modulated using independent dual polarization IQ modulators. The modulators were fed by 30Gbaud of DP-QPSK (Nyquist pulse shaped with roll-off factor of 0.1) generated by an arbitrary wave generator operating at 60GSa/s and a  $2^{15}-1$  pseudorandom binary sequence (PRBS). The AWG decorrelated the modulating data for X and Y polarizations by 4096 symbols. The output of the two modulators then were further decorrelated by an optical path difference of 4m before combination, which generated 30 channels each of which was decorrelated from its two neighboring channels. The optical spectrum at the output of the transmitter can be seen in Fig. 1(b).

### 3. Dual-band, polarization insensitive OPC

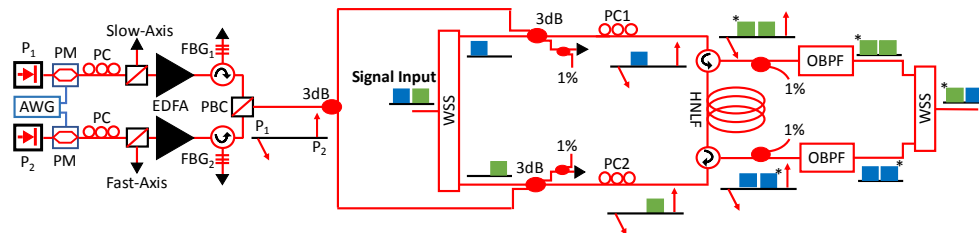


Fig. 2. Experimental setup of dual-band, polarization insensitive, dual pump OPC. AWG: arbitrary waveform generator, PM: phase modulator, PC: polarization controller, FBG: fiber Bragg grating, PBC: polarization beam combiner, WSS: wavelength selective switch, HNLF: highly nonlinear fiber, OBPF: optical band-pass filter.

Figure 2 shows the polarization insensitive dual-band OPC with orthogonally polarized pumps spectrally located at ( $P_1$ )1540.4nm and ( $P_2$ )1570.1nm. The two pump lasers (linewidth<10kHz) were counter dithered (phase modulated) with two tones (60MHz and 600MHz) to raise the effective Brillouin threshold of the highly nonlinear fiber (HNLF) by 8dB. The phases of the electrical RF tones for each optical phase modulator were calibrated to minimize the phase modulation transfer from the pumps to the idlers of the OPC. A phase modulation suppression of 32dBc was observed when conjugating a continuous wave (CW) laser. A polarization controller (PC) and polarization beam splitter were used to enhance the degree of polarization of the two pumps. The two pump lasers were amplified using C-band high power EDFA (to amplify  $P_1$ ) and L-band high power EDFA (to amplify  $P_2$ ), then the amplified pumps were filtered using circulator and fiber Bragg grating (FBG) and combined using a polarization beam combiner (PBC). Finally, two copies of the perpendicularly polarized pumps were created (using a 3dB splitter). At the signal input to the dual-band OPC, a WSS was used to split the input signals into the two bands, the blue band (1541nm-1555.7nm) and the green band (1555.7nm-1570.4nm), as shown in Fig. 2. A 3dB coupler was used to combine each signal band with a copy of the perpendicularly polarized pumps. A polarization controller was installed on each path to align the pumps with the principal axis of the HNLF, to minimize polarization walk-off and so optimize the polarization independence of the conjugation process. The two bands combined with the pumps were counter propagated in the HNLF ( $L = 100\text{m}$ ,  $\lambda_0 = 1557\text{nm}$ ,  $\gamma_0 = 28/\text{W}/\text{km}$ ,  $S = 0.024\text{ps}/\text{nm}^2/\text{km}$ ) via two circulators, as shown in Fig. 2. Each propagation direction along the HNLF formed an independent OPC, one for each band (the blue and green bands in Fig. 2). The circulators enabled the extraction of signals, conjugates and pumps after passing through the HNLF. Tunable optical band pass filters (OBPFs) were used to remove the high-power pumps from the output of each OPC. Finally, a WSS was used at the output of the OPC to filter, gain equalize and combine the two conjugated bands.

Figure 3(a) shows the optical spectrum at the output monitor (1%) of each OPC path (OPC1 and OPC2), where both paths conjugate an optical signal band of the modulated signal

(15 channels) simultaneously. From the figure, it can be seen that the modulated channels were conjugated with conversion efficiencies ranging around  $-6\text{dB}$ . Figure 3(b) shows the error vector magnitude ( $EVM^2$  [dB]) as a function of the received OSNR for signals in back-to-back and conjugated through the OPC, showing the performance of the central channel from each band (Channel 8 and Channel 23). Each point in Fig. 3(b) represents the mean of  $EVM^2$  for 10 traces, each containing 500000 samples, detected by 100GSa/s coherent dual polarization optical receiver. The back-to-back measurement (bypassing the OPC) shows that the performance saturated at an  $EVM^2$  of  $-18.7\text{dB}$  at the highest OSNR ( $30.1\text{dB}$ ) due to the transceiver noise and interference from neighboring channels. With the OPC, the maximum received OSNR was degraded by  $3.5\text{dB}$  due to the extra ASE noise added by the OPC. Otherwise, the performance of the dual polarized conjugated signals matched the performance of the unconjugated signals.

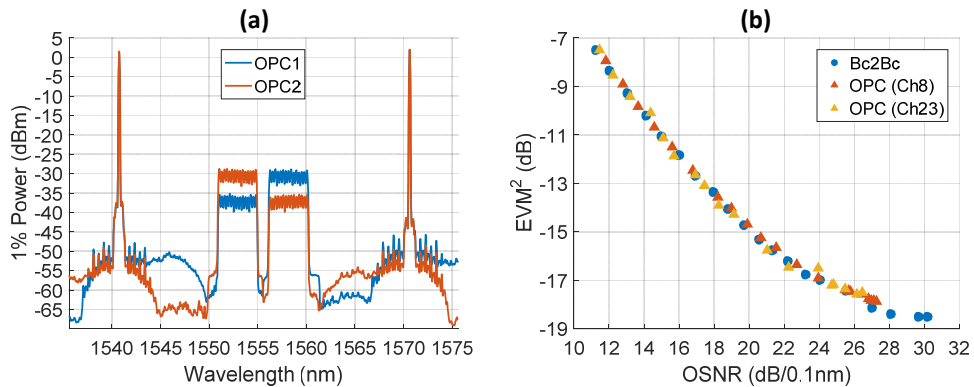


Fig. 3. (a) Optical spectrum at the output monitor points of the OPC (on both paths). (b) Received  $EVM^2$  (dB) factor as a function of OSNR. Bc2Bc: back-to-back.

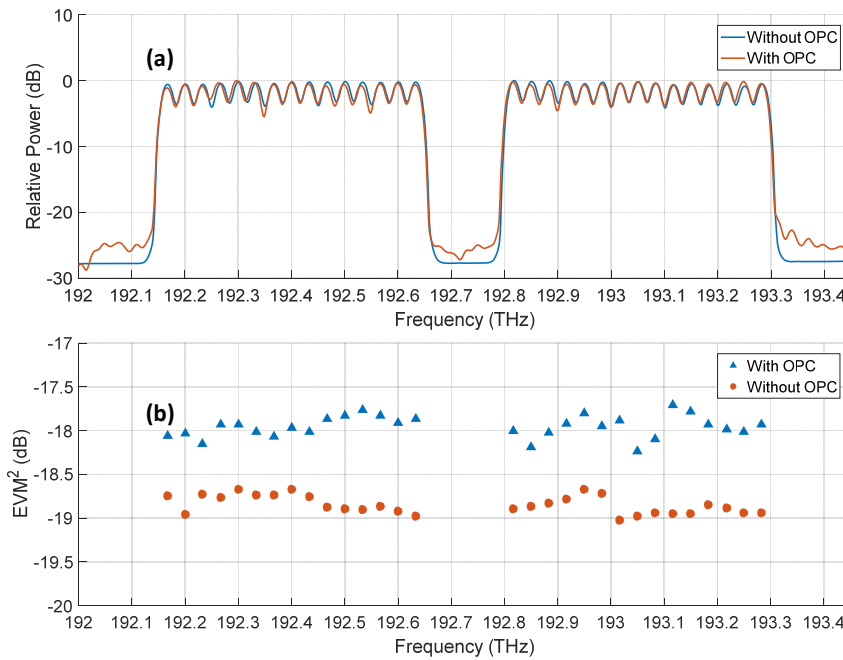


Fig. 4. (a) Optical spectrum with and without OPC, at maximum OSNR. (b)  $EVM^2$  (dB) of the individual channels with and without OPC, at maximum OSNR.

Figure 4 shows the spectral properties (a) and the maximum  $EVM^2$  (b) of the 30 modulated channels (back-to-back and conjugated through the OPC). The maximum achieved OSNR is degraded by around 3.2dB, whilst the  $EVM^2$  shows a degradation  $\sim 0.8$ dB. The variation in performance among the different channels is below 0.6dB in both cases.

#### 4. Recirculating loop

To emulate a long-haul optical transmission system, we have implemented a recirculating loop that deployed two 50km spans with backward pumped distributed 1st order Raman amplification, shown in Fig. 5. The modulated signals (see section 2) were switched into the loop using a 2x1 optical switch (SW1). A 3dB coupler was used to split the signal into two copies, one bypassing the OPC and one passing through the OPC to generate the conjugates of the two bands simultaneously. The OPC path contained two additional EDFAs to overcome the 22dB net insertion loss of the OPC block (section 3). A second 2x1 optical switch (SW2) was used to switch between the signals bypassing the OPC and the conjugated signals, to emulate the deployment of OPC within the transmission link. At the output of SW2, an EDFA (NF = 6dB) was used to boost and control the signal power injected to the first distributed Raman span of (50km) standard single mode fiber (Sterlite G.652.D). A 3dB splitter was used to create two equal powered copies of the 1455nm Raman pump and then injected in the backward propagation direction of each 50km span using a wavelength division multiplexer (WDM). At the output of the first span, a gain flattening filter (GFF) was used to maintain the spectral flatness of the signals. An EDFA (at the output of the GFF) was used to compensate for the WDM's and the GFF's insertion loss, then the modulated signals propagate through the second distributed Raman span. At the output of the second span, a 3dB splitter was used to direct a copy of the transmitted signals to the coherent receiver. The Raman pumping power was adjusted for each signal launch powers to achieve zero net dB gain (avoiding the effect of Raman pump depletion at high signals powers), the power profile measured for both spans and displayed in Fig. 5(b). The received signals were then processed using commercial digital signal processing (DSP) software (Tektronix OM4245); at which used a constant modulus algorithm (CMA) to optimize a 7 taps polarization demultiplexer. The value of dispersion compensated in the DSP was dependent on the system length (number of spans) and whether a mid-link OPC was emulated in the link. In OPC assisted system, the DSP compensated only for the residual dispersion resulted from the dispersion slope and the wavelength shift of the OPC. The receiver then quantified the received signal quality: BER (from decoded bit sequence) and EVM (from the constellation). The number of OPCs deployed along the system and their location along the emulated link was controlled by changing the frequency at which SW2 passed the signal conjugates into the loop. The OPCs were located symmetrically along the link with double segmented separation between any two consecutive OPCs [9] (in case of multiple OPCs), which means that the number of spans between the transmitter/receiver and the nearest OPC is half the number of spans between two consecutive OPCs, as shown in Fig. 5(c).

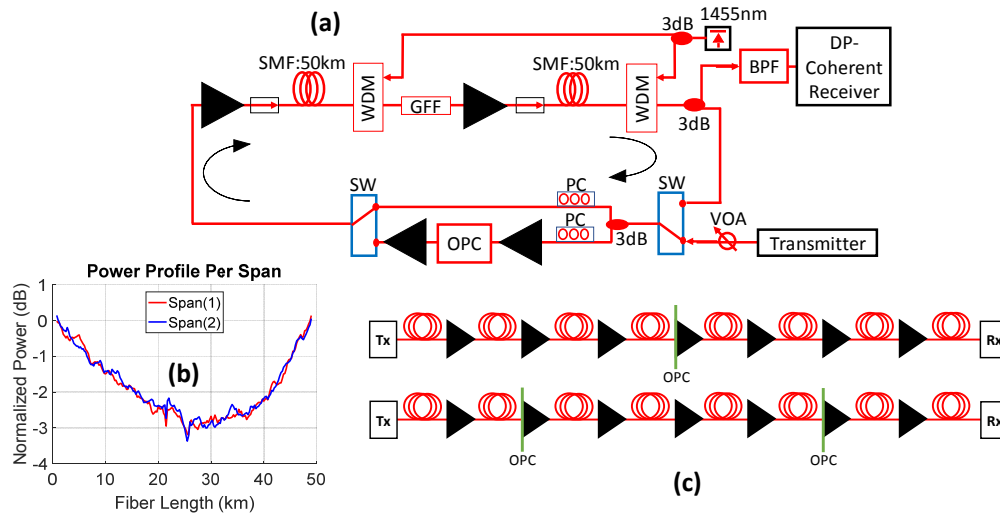


Fig. 5. (a) Experimental setup of OPC assisted distributed Raman amplified transmission system. (b) Normalized power profile of signals propagating through the two 1st order distributed Raman amplified spans. (c) Multi-OPC deployment technique. VOA: variable optical attenuator, SW: switch, PC: polarization controller, SMF: single mode fiber, WDM: wavelength-division multiplexer, GFF: gain flattening filter, BPF: band-pass filter.

### 5. Results and discussion

Figure 6 shows the  $EVM^2$  as a function of signal power launched into the distributed Raman amplified spans at a transmission distance of 2,400km plotting the performance of the central channel of each band (channel 8 and channel 23) with between zero and three OPCs. Without OPC, the electronically dispersion compensated (EDC) system reaches its minimum  $EVM^2$  (-11.6dB) at per channel launch power of approximately -3dBm, while a single mid-link OPC improves in the optimum  $EVM^2$  by 2.2dB as confirmed by the constellation of the received 30GBaud DP-QPSK signal. The level of improvement suggests that 89% of the deterministic nonlinear signal-signal interactions were compensated by the OPC, based on the cubic relationship between the optimum SNR and residual nonlinearity [23]. As the number of OPCs increases, the nonlinear threshold (power at minimum  $EVM^2$ ) is reduced. The reduction in nonlinear threshold is 0.7dB for two OPCs and 1.1dB for three OPCs, whilst the performance is degraded by 0.6dB and 0.8dB, respectively.

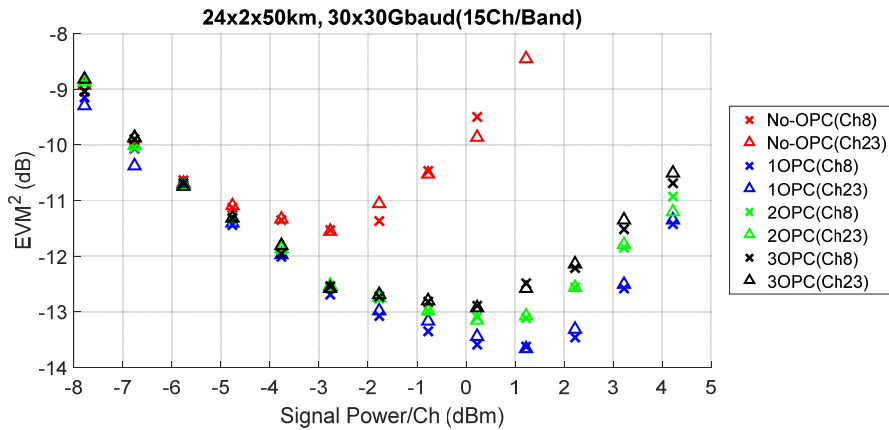


Fig. 6.  $EVM^2$  as a function of signal power at the optimum signal power measured at 2400km without OPC, 1-OPC, 2-OPC, and 3-OPC.

It has been proposed that power symmetry [12] and polarization mode dispersion [20] will both impact the performance of OPC based transmission systems. In our case, we measured a power symmetry of better than 89% and the theoretically predicted reduction in compensation efficiency due to PMD (assuming a PMD coefficient of  $0.04\text{ps}/\text{km}^{0.5}$ ) of approximately 4% neglecting inter-band nonlinearity. However, these reductions in compensation efficiency are insufficient to explain why the use of multiple OPCs degrades the performance. Such a reversal is only possible due to excess noise [15] (negligible in our case) or enhanced nonlinear phase matching due to the effective dispersion management provided by OPC [9], implying that the residual nonlinearity in the weakly phase matched region will increase quadratically with the number of OPCs. The uncompensated nonlinear noise in this experiment may be a result of inter-band nonlinearities that may have been compensated due to the band filtering within the OPC.

Figure 7 shows the  $EVM^2$  (for the central channel of each band) as a function of distance for an EDC system and a system that deploys a mid-link OPC. The figure shows a clear advantage of the mid-link OPC assisted system over the EDC system, enhancing the maximum transmission distance by 72% (at  $EVM^2$  threshold of 9dB). For a given realistic system, the reach enhancement (achieved by OPC) is expected to be length dependent. At short distances, the dominance of transceiver noise limits the maximum achievable performance of the demodulated signals (at the receiver side), which can be seen in Fig. 3(b) as the performance (EVM) saturates when the OSNR is ranging above 26dB. As a result, the performance enhancement achieved by the OPC will be limited by the maximum achievable performance (limited by transceiver noise). This limited performance enhancement of the OPC can be seen in Fig. 7 as the OPC achieves only 0.6dB performance enhancement at 1200km. At higher distance, the total (linear and nonlinear) noise generated from the transmission link starts to grow and dominate over the transceiver noise; in this case the OPC compensates for the nonlinear noise of the link and results a constant performance enhancement of 2.35dB (72%) at distances above 3000km, as can be seen in Fig. 7. Figure 8 shows the optical spectrum and the BER for each channel measured at the maximum distance (compatible with HD-RS(255,239), pre-FEC BER =  $3.15 \times 10^{-3}$  [24]). The results confirm that the distance enhancement achieved by the mid-link OPC applies to all 30 channels, increasing the 4400km reach to 7600km (72%).

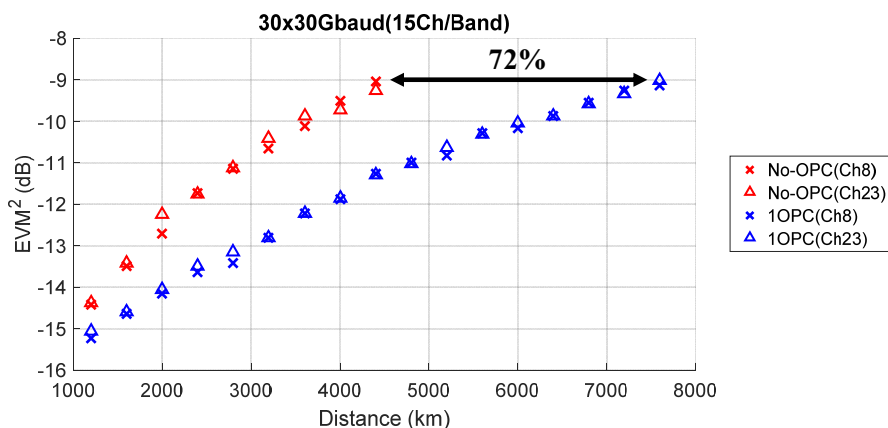


Fig. 7.  $EVM^2$  (in dB) as a function of distance.

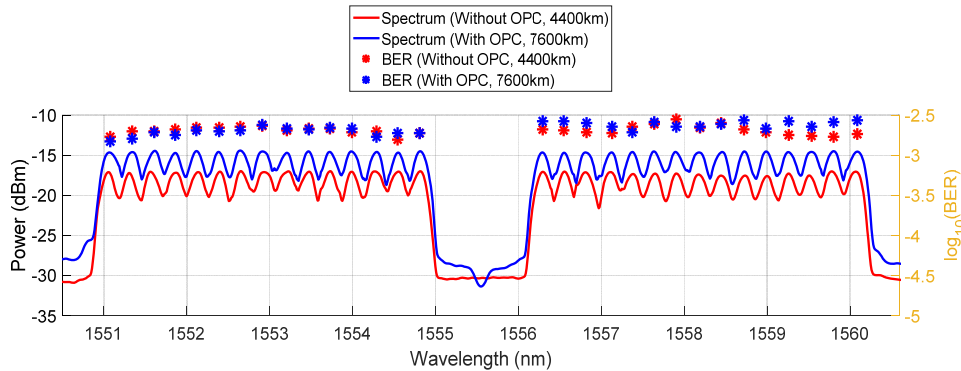


Fig. 8. Optical spectrum (resolution 0.1nm) and BER per channel of the received signals at the maximum distance of EDC system and mid-link OPC assisted system.

## Conclusions

In this paper we have experimentally demonstrated a mid-link OPC assisted distributed Raman amplified transmission system that achieves significant performance enhancement (2.3dB) of WDM signals spread over optical bandwidth of 1THz (two bands, 500GHz each, that contain 30x30Gbaud PM-QPSK signals, Spectral Efficiency = 3.6b/s/Hz). The distributed Raman amplification in the reported experiment has achieved 89% nonlinearity compensation of the deterministic signal-signal nonlinear interactions. We have shown that the implemented system is still limited by the uncompensated (10%) deterministic nonlinear signal-signal interactions; as increasing the number of OPCs, 2 and 3 OPCs, have resulted in a degradation in the performance enhancement achieved by a single OPC of 0.6dB and 0.8dB, respectively. Compared to long-haul experimental demonstrations reported in the literature, our results provide a greater reach enhancement: we have achieved a 72% enhancement using mid-link OPC compared to an EDC system.

Original data for this work is available through Aston Research Explorer (<https://doi.org/10.17036/researchdata.aston.ac.uk.00000354>).

## Funding

Engineering and Physical Sciences Research Council (EPSRC) (EP/J017582/1 [UNLOC], EP/L000091/1 [PEACE]); and Marie Curie Initial Training Networks (FP7 ITN) (608099 [ICONE]).

## Acknowledgments

We would like to thank Dr. Marc Stephens for the useful discussions. Also, we thank Sterlite Technologies for providing the transmission fiber, and Finisar for providing a wavelength selective switch.